

THE UTILITY OF TOTAL LIGHTNING IN CONVECTIVE NOWCASTING

Nicholas L. Wilson
University of Oklahoma, Norman, Oklahoma, USA

Daniel W. Breed and Thomas R. Saxen
National Center for Atmospheric Research, Boulder, Colorado, USA

Nicholas W. S. Demetriades
Vaisala, Inc., Tucson, Arizona, USA

1. INTRODUCTION

The demand for precise forecasts by national government agencies, private industry and the general public have heightened the pressure upon the meteorology community to improve the performance of high-resolution thunderstorm forecasts known as “convective nowcasts”. Nowcasting serves as a bridge between current weather and mesoscale forecasting techniques, which rely heavily upon numerical weather prediction for 3-to-48 hour regional guidance (e.g. RUC, MM5 and WRF in the United States). The goal of a convective nowcast is to provide time- and place-specific forecasts of thunderstorm initiation, movement, growth and decay, and severe weather potential. The temporal resolution of a convective nowcast exists from a few tens of minutes until three-to-six hours, but the skill of current nowcast products deteriorates quickly beyond one hour (Dabberdt, 2001).

State-of-the-art observation equipment, expert systems, conceptual models and forecaster involvement are all integral components of any successful convective nowcast. The nowcast method varies upon the geographic location, intended applications and needs the end-users wish to fulfill. For example, thunderstorm initiation and convective mode differ greatly between the high plains of the leeward Rocky Mountains and the moisture-laden boundary layers found along the United States’ Gulf of Mexico coastal areas. Similarly, the National Weather Service (NWS) has different obligations to fulfill with its nowcast, as opposed to utility companies that are concerned with protecting their own operational assets. Despite these inherent differences, the common bond between each convective nowcast is the dependence upon observations with high spatial and temporal resolution. Observations have traditionally been provided by weather radar, surface mesonets, cloud-to-ground lightning detection,

wind profilers, radiosondes and satellites. We now introduce three-dimensional total lightning (cloud plus cloud-to-ground) mapping into the convective storm nowcasting process. Data are used from Vaisala, Inc.’s second-generation Lightning Detection and Ranging (LDAR II) VHF time-of-arrival network in the Dallas-Ft. Worth, Texas area (Demetriades et al., 2002).

Expert systems are also vital components toward the nowcast process. They create deterministic output derived from observational networks in a matter of seconds, not possible by human analysis alone. One such example is the NCAR Auto-Nowcast system (ANC; Mueller et al., 2003), which was deployed to the Ft. Worth, Texas NWS forecast office in March 2005 as part of the NWS’ two-year “Man in the Loop” nowcasting demonstration (Nelson et al., 2005). The ANC is an interactive software package that integrates multiple meteorological datasets in real-time and uses fuzzy logic to combine them and create 60-minute forecasts of thunderstorm initiation, growth and decay every five minutes. The co-location of LDAR II and the ANC allows for the evaluation of various nowcasting applications derived from total lightning. The Dallas-Ft. Worth ANC datasets include: level II data from 7 WSR-88D radars across the southern plains, observed and derived satellite data, METAR and surface mesonet observations, automated feature detection algorithms, a boundary layer model (VDRAS; Sun and Crook, 2001), RUC-20 gridded NWP output and now LDAR II total lightning.

This paper introduces the method in which total lightning is integrated into the ANC and provides the quantitative forecast verification results using cases archived from spring-summer 2005. Additional nowcasting techniques are discussed as well, including the use of total lightning coverage and frequency trends to forecast future thunderstorm intensity and the estimation of

thunderstorm echo tops using VHF source heights from LDAR II. The results demonstrate that the use of VHF total lightning improves convective nowcast performance in the 0-to-60 minute forecast period.

2. DALLAS - FT. WORTH RESEARCH DOMAIN FOR NOWCASTING

Dallas-Ft. Worth total lightning data have been available in real-time from LDAR II since 2001. LDAR II is an array of 7 sensors centered at Dallas-Ft. Worth International Airport with an average radial baseline of 20 to 30 km (Fig. 1). The sensors passively measure radiation emitted by electrical processes and locate the sources of the radiation to produce three-dimensional mapping of all lightning activity. Real-time data are received at Vaisala, Inc.'s Tucson office where post-processing occurs. Two-minute data segments are then transmitted to the NWS Southern Region Headquarters in Ft. Worth for dispersal to its forecast offices. NWS Ft. Worth forecasters often utilize the LDAR II total lightning products in AWIPS to assist with the nowcast of thunderstorms and severe weather within their county warning area.

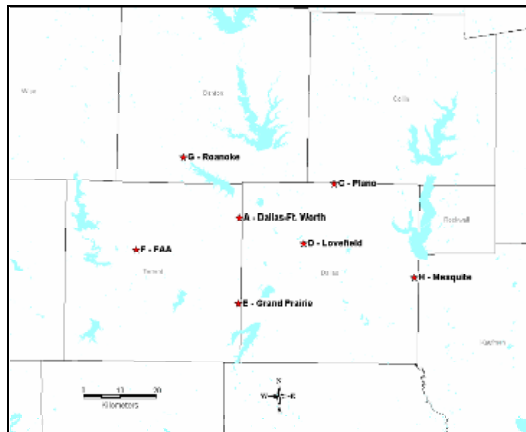


Figure 1. Locations of the Dallas-Ft. Worth LDAR II sites (stars). Sensor A is located at DFW International Airport. Local lakes and county lines are also shown.

The ANC was originally developed in 1995, as an expert system to assist forecasters with the daunting process of making important decisions under pressure and time constraints. The ANC is designed to perform best with forecaster interaction during the nowcast process. Forecasters have the ability to enter boundary locations and motion

vectors that assist the fuzzy logic engine in identifying areas of possible convective initiation. Since the presence of lightning indicates a thunderstorm is already present, the implementation of LDAR II total lightning is limited to the ANC's growth/decay and extrapolation component. We will evaluate its potential to improve the quantitative skill of thunderstorm growth and decay nowcasts in Section 6.

3. WEATHER RADAR AND NOWCASTING

Since the ability to sense meteorological echoes with military radar was discovered during WW II (Maynard, 1945), weather radar has become the primary tool used for convective nowcasting. The ability to remotely sense precipitation intensity and the movement of thunderstorm cells are key components for a successful nowcast. Two popular algorithms are used to identify and track the characteristics of storm cells over time in a Lagrangian fashion with weather radar. Storm Cell Identification and Tracking (SCIT; Johnson et al., 1998) uses a mass-weighted centroid and 7 radar reflectivity (dBZ) thresholds to identify, characterize, track and forecast the short-term movement of storm cells identified in three dimensions. Similarly, the Thunderstorm, Identification, Tracking, Analysis, and Nowcasting (TITAN; Dixon and Weiner, 1993) algorithm identifies two- or three-dimensional storm cell centroids using radar reflectivity (dBZ) thresholds, but uses cross-correlation techniques to forecast movement. TITAN's algorithms are used within the Dallas-Ft. Worth ANC's cell growth/decay and extrapolation component. The ANC uses TITAN to define contiguous regions of radar reflectivity into individual thunderstorm cells using area and intensity thresholds. TITAN tracks the identified storms, calculating various trend attributes for each cell.

There are inherent disadvantages that exist when only using weather radar for convective nowcasting guidance. First, it is difficult to identify individual updraft impulses that lead to new storm development using only radar reflectivity. This often occurs during multicell thunderstorm events characterized by low-shear environments. Secondly, weather radar does not capture the entire volume of a thunderstorm when it is in close range. The extensive WSR-88D network allows for multi-radar solutions in the United States, but other

parts of the world with minimal radar infrastructure suffer. Weather radars are typically placed near population centers, so observational data is often compromised in circumstances such as this when its use is most crucial. Conversely, at long ranges the SCIT echo top altitude trends are inaccurate at long ranges when thunderstorm echo tops move between beam-scanning elevation angles, which can exaggerate storm growth and/or decay. Lastly, the 5-minute volume scans of the WSR-88D network are not frequent enough to capture the dynamic evolution of severe thunderstorms.

Even when weather radar products are satisfactory, trends of its information have offered mixed results. Mackeen et al. (1999) found that radar-reflectivity derived storm cell trends are poorly related to the remaining lifetime in a thunderstorm. Additionally, Howard et al. (1997) suggest that discrepancies in the volume scan strategy and radar range can greatly effect the trending of radar-derived storm-based trends and should be taken into account when developing relationships to assist with nowcasting.

The poor performance of weather radar trending may be understood once examining the physical representation of radar reflectivity. Weather radar reflectivity data are a measure of the backscatter of hydrometeors produced by convection, as opposed to the convective process itself. Thus, reflectivity data are the result of convective processes integrated across the temporal resolution of the volume scan. Mackeen et al. (1997) also suggest that radar reflectivity used in conjunction with other data sources could better capture convective processes in a statistical manner. Considering the ANC has only used radar reflectivity data to forecast growth/decay and extrapolation of convection since its inception, the integration of another data source (e.g. LDAR II total lightning) would likely improve its nowcasting skill.

Harlin et al. (2000), Lang and Rutledge (2002), MacGorman et al. (2002) and Steiger et al. (2005) have all conducted analysis which indicates that total lightning characteristics are correlated well with the evolution of thunderstorm intensity. Dotzek et al. (2001) note from observations that there is very little lag time between changes in the upper-storm bulk microphysics and electrical activity. Total lightning appears to capture the dynamical and microphysical development of thunderstorms in near real-time. Since total lightning data are

better connected to convective processes, it is hypothesized that trends of total lightning will outperform those of radar reflectivity when nowcasting thunderstorm growth and decay in the ANC.

4. FLASH EXTENT DENSITY

Flash Extent Density (FED; Lojou and Cummins, 2005) is used to depict total lightning activity from the LDAR II for our applications created for the Dallas-Ft. Worth ANC. It employs a "branched segment" reconstruction of the lightning flash using temporal and spatial constraints upon VHF sources created by the electrical breakdown in propagation of mostly negative and some positive leaders. FED helps to normalize the effect of decreasing VHF source detection efficiency with range because flash detection efficiency decreases at a much slower rate with increasing distance from the center of the LDAR II network. Flash detection efficiency is 95% within the network and better than 90% out to a range of 120 km. A 1 km² Cartesian grid box obtains a "hit" every time a reconstructed branch passes thru its boundaries. The FED representation was chosen for the ANC because of its similarities in shape, appearance and structure to that of traditional radar reflectivity, allowing for easy implementation of TITAN's algorithms (Fig. 2).

Before developing thunderstorm growth/decay relationships from FED data, a conceptual model of the physical processes it represents is examined. Proctor (1991) and Steiger et al. (2005) found that total lightning flash initiation points are usually in areas of radar reflectivity gradient on the outskirts of the main precipitation core. It is hypothesized that reflectivity gradients are a proxy for gradients in vertical velocity, where charge separation would be the greatest. The favored reflectivity gradient for flash initiation and propagation is downshear of the main updraft and reflectivity core, demonstrating that charge is advected on the hydrometeors in environments of significant wind shear (e.g. supercells). Demetriades et al. (2003) found that the base reflectivity area of precipitation greater than 20 dBZ is nearly equivalent in the area encompassed by the VHF source densities, with Steiger et al. (2005) showing that these are offset anywhere from 5-to-15 km depending on advection of hydrometeors by the mean wind. Since a sufficient amount of time is necessary to build up enough

electrical charge within a convective cell to produce lightning, it is not unusual that most of the LDAR II source activity is associated with mature-to-dissipating convective cells. Saunders (1993) noted that as a thunderstorm's updraft intensifies, precipitation particles are lofted higher, especially the lighter ice crystals that are typically charged positively. Thus, the negative leader bias of the LDAR II is quite successful at capturing flashes that propagate through positively charged anvil regions (Fig. 2). Likewise, mesoscale convective systems that transport descending ice crystals into the stratiform precipitation region are well-captured by LDAR II. Demetriades et al. (2005) observed many cloud flashes that initiated in the leading convective line and propagated into the stratiform region, occasionally in association with high amplitude cloud-to-ground flashes.

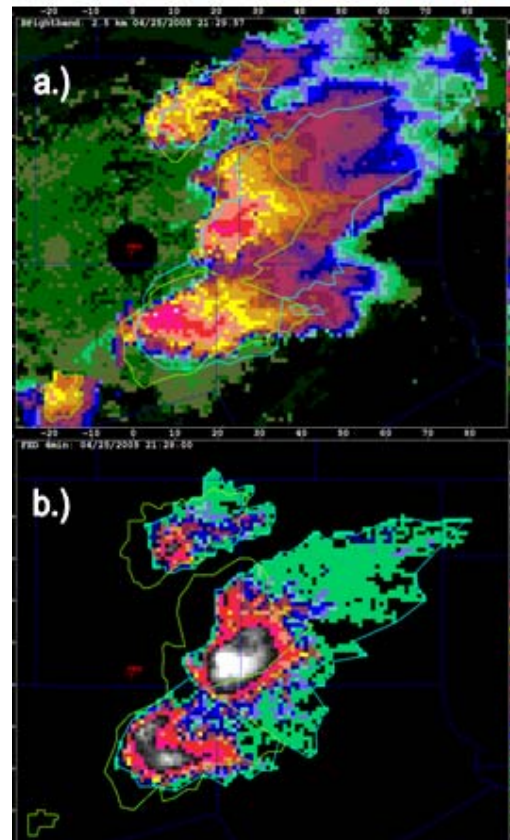


Figure 2. a.) 2.5 km CAPPI of radar reflectivity (dBZ) from the KFWWSR-88D at 2130 UTC on 25 April 2005. The overlaid yellow boundaries distinguish the >35 dBZ threshold TITAN cells, while the cyan boundaries distinguish the >0.25 flashes $\text{km}^{-2} \text{min}^{-1}$ TITAN cells. b.) Same window, except now the corresponding FED (flashes $\text{km}^{-2} \text{min}^{-1}$) activity in the Dallas Co. cell extends 40 km downshear from the main precipitation core through the positively charged anvil.

5. TITAN-DERIVED STORM ATTRIBUTES

Three TITAN-derived storm cell attributes for both radar reflectivity and total lightning cells have been tracked for this study, including: maximum dBZ or FED, storm cell area and storm cell normalized area growth rate. The maximum dBZ or FED value is simply the largest value within the boundary of the identified storm cell. The storm cell area is area of the composite reflectivity or FED above a certain threshold value in units of km^2 . Lastly, the normalized area growth rate (NAGR) is a weighted history of the identified cell's area, taking into account the last five sets of data. Thus, the past 25-to-30 minutes

of radar information and 16 minutes of LDAR II data are considered.

The purpose of the ANC's growth/decay and extrapolation component is to predict whether a TITAN-derived 35 dBZ threshold storm cell will grow, maintain its current area, or dissipate 60 minutes from the forecast time. Using this as a starting point, we took six different TITAN-derived attributes from radar reflectivity and FED identified storms and evaluated their skill at forecasting the 35 dBZ threshold storm cell area in 5-minute intervals from 0-70 minutes from forecast time. The Pearson linear lag correlation coefficient (r) has been calculated at each time iteration and averaged over the 15 cases in the dataset from spring-summer 2005 that traversed the Dallas-Ft. Worth area.

In Figures 3-6, the abscissa is aligned at $r = 0.3$, which is the widely used threshold to determine if a significant physical relationship exists between the two parameters of concern. The values of r are lower than expected, due in part to the wide variations that exist with TITAN's NAGR and 35 dBZ threshold storm cell area parameter calculations between observation times. Additionally, all parameters were normalized to the nearest 5-minute increment to conduct the correlation analysis between datasets of varying temporal resolutions, possibly leading to decreased values of r .

The lag correlations in Figure 3 illustrate that TITAN-derived 35 dBZ threshold NAGR is a better nowcast tool in the 0-to-30 minute range. However, the TITAN-derived 0.25 flashes $\text{km}^{-2} \text{min}^{-1}$ threshold NAGR offers improved performance at 40 minutes and beyond, including an impressive $r = 0.299$ at the 55-minute forecast verification time.

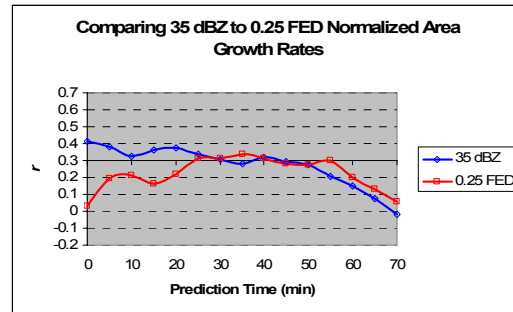


Figure 3. The Pearson linear lag correlation coefficients in 5-min intervals comparing the TITAN 35 dBZ cell NAGR (blue) to the TITAN 0.25 FED cell (red) as predictors for the 35 dBZ cell area. The lag correlations are calculated for each of the 15 thunderstorms in the dataset and then averaged together at 5-min iterations.

In Figure 4, the NAGR trends of the storm cells' convective cores are explored using a 45 dBZ and 1.0 flashes $\text{km}^{-2} \text{min}^{-1}$ threshold for the TITAN-derived radar reflectivity NAGR and FED NAGR respectively. The nowcast parameters do not perform as well as their prior counterparts, but a similar relationship is exhibited between the radar and total lightning data. The TITAN-derived radar reflectivity NAGR is a better nowcast tool in the 0-to-35 minute range. However, the TITAN-derived FED NAGR once again offers improved nowcasting performance at 40 minutes and beyond. In fact, beyond 45 minutes, the r for the TITAN-derived radar reflectivity NAGR drops below zero. The inclusion of this field in the Dallas-Ft. Worth ANC likely degrades the performance of its growth/decay forecast component.

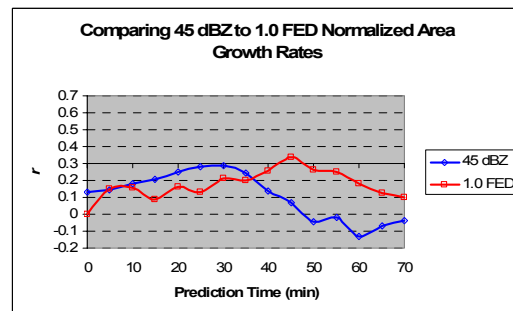


Figure 4. Same as Figure 3, except now comparing the TITAN 45 dBZ NAGR (blue) to the TITAN 1.0 FED NAGR (red).

Figure 5 illustrates the Pearson linear lag correlation coefficient when using the TITAN-derived maximum reflectivity and FED to nowcast the future 35 dBZ threshold storm cell area. At forecast time the maximum reflectivity of a storm is very well correlated with its corresponding area ($r = 0.599$), however the relationship quickly deteriorates beyond 20 minutes from forecast time. The TITAN-derived maximum FED is a better nowcast tool at 30 minutes and beyond, although neither is well correlated to the 35 dBZ threshold storm cell area.

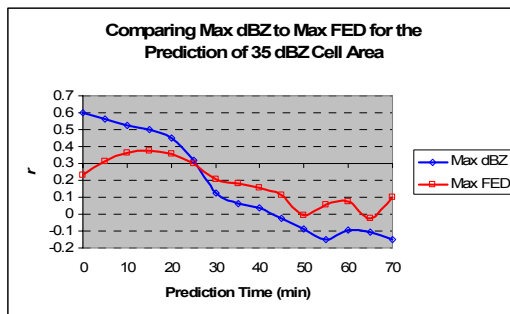


Figure 5. Same as Figure 3, except now comparing the TITAN maximum radar reflectivity (dBZ; blue) to the TITAN maximum FED (red).

The results from Figures 3-5 demonstrate that TITAN-derived total lightning trends have great potential to improve nowcasts in the 40-to-60 minute timeframe. Lead times on the order of nearly an hour without the assistance of numerical weather prediction hold value for the improvement of the ANC's 60-minute thunderstorm growth/decay forecast output.

Although not currently a feature included in the ANC, the abilities of the same TITAN-derived fields have been examined to improve the nowcast of thunderstorm intensity as well. Pearson linear lag correlation coefficients are calculated using TITAN-derived 35 dBZ, 45 dBZ, 0.25 flashes $\text{km}^{-2} \text{min}^{-1}$ and 1.0 flashes $\text{km}^{-2} \text{min}^{-1}$ threshold NAGRs to predict the maximum reflectivity in the same storm cell, 0-to-60 minutes from forecast time using the identical dataset (Fig. 6). The results show similar trends, with the TITAN-derived radar reflectivity parameters performing best in the first 15 minutes. Thereafter, the 0.25 flashes $\text{km}^{-2} \text{min}^{-1}$ threshold NAGR exhibits the best performance. Its r exceeds 0.4 for forecasts between 25 and 40 minutes. At the 60-minute forecast verification the FED trends ($r = 0.15$ to 0.20) are better predictors of thunderstorm intensity than the radar reflectivity trends.

These Pearson linear lag correlation coefficients are similar to those seen with the forecast of storm cell area. In addition, the 35 dBZ and 0.25 flashes $\text{km}^{-2} \text{min}^{-1}$ threshold cells outperform their 45 dBZ and 1.0 flashes $\text{km}^{-2} \text{min}^{-1}$ threshold counterparts. This indicates that identifying larger storm cells as a result of lower thresholds is beneficial for both the radar reflectivity and total lightning data when conducting attribute analysis for nowcasting.

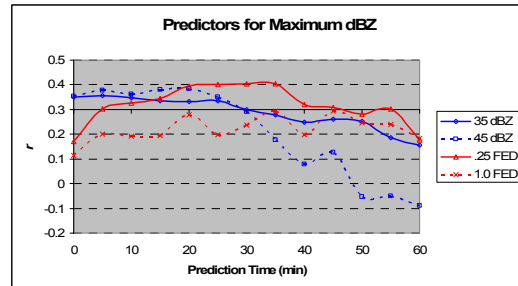


Figure 6. Same as Figure 3, except now comparing the TITAN 35 dBZ NAGR, TITAN 45 dBZ NAGR, TITAN 0.25 FED NAGR, and TITAN 1.0 FED NAGR as predictors for the TITAN maximum reflectivity.

6. TOTAL LIGHTNING IN THE NCAR AUTO-NOWCAST SYSTEM

6.1 Method

The strong performance of TITAN-derived total lightning cell attribute trends provides confidence that they can improve the overall skill of the ANC's growth/decay and extrapolation component. The ANC uses a fuzzy logic engine to combine multiple TITAN-derived cell trend attributes into a final deterministic nowcast of cell area growth, maintenance or decay. The key components of any fuzzy logic based system are the membership functions. A membership function defines the "degree of truthness" of a certain parameter. The ANC is the ideal framework to use fuzzy logic with its various datasets and the non-binary decision making necessary to create a nowcast. The growth and decay component of the ANC uses membership functions weighted from -1 to 1 for TITAN-derived cell attributes. Negative values indicate cell decay, values near zero indicate maintenance of cell area and values near one indicate cell growth.

Two total lightning functions from TITAN-derived attributes have been developed for testing in the ANC. The first is the 0.25

flashes $\text{km}^{-2} \text{min}^{-1}$ threshold history-weighted NAGR (Fig. 7). The other total lightning membership function that has been developed is the maximum FED value (Fig. 8). The inflection point that differentiates growth and decay for each was optimized using the Heidke Skill Score (Heidke, 1926) from the training set of 15 storm cells that tracked in vicinity of the LDAR II network. These two total lightning relationships join the four legacy membership functions derived from surface observations and radar reflectivity used in the ANC's growth/decay component since its inception. A more detailed explanation of the ANC's fuzzy logic set-up and implementation can be found in Wilson et al. (2006).

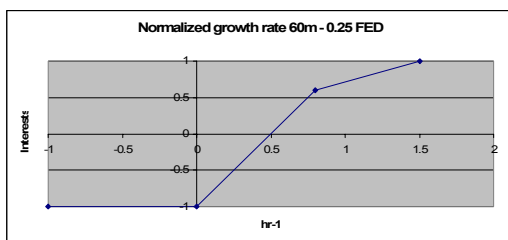


Figure 7. The membership function for the TITAN-derived 0.25 flashes $\text{km}^{-2} \text{min}^{-1}$ threshold NAGR (normalized growth hr^{-1}).

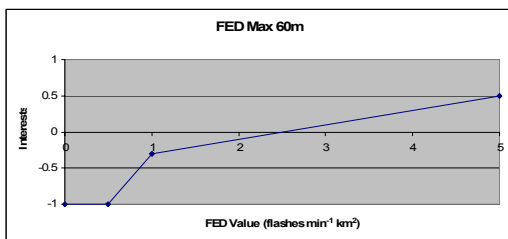


Figure 8. Same as Figure 7, except now for the maximum FED value.

6.2 25 May 2005 example case

A squall line approached the Dallas-Ft. Worth area from the northwest on this day at 1600 UTC. CAPE vales near 800 J kg^{-1} and 30 kt steering flow characterized the event. Moderate lightning activity accompanied these non-severe thunderstorms as they passed through Dallas County. Peak total lightning activity up to $11 \text{ flashes min}^{-1} \text{ km}^{-2}$ was observed in the main line at 1910 UTC. Additional isolated convective cells developed on the southern flank of the squall line around 1900 UTC. Moderate lightning activity of $8.25 \text{ flashes min}^{-1} \text{ km}^{-2}$ accompanied a cell to the south of Dallas at 1910 UTC before it weakened considerably. The squall line and

associated convective cells departed the NWS Ft. Worth CWA by 2200 UTC. An example of the ANC forecast output and subsequent verification are provided below (Fig. 9-10).

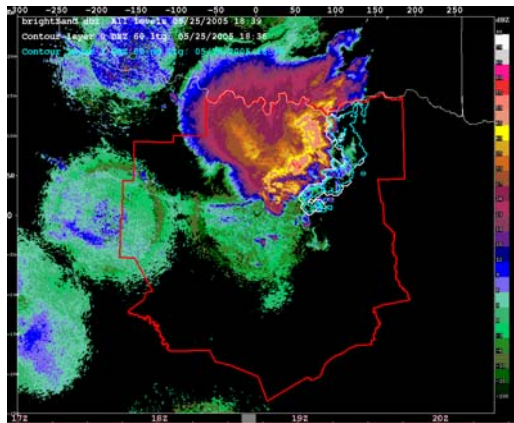


Figure 9. The 60-minute ANC forecast output on 25 May 2005 at 1836 UTC. The cyan boundaries are the forecasted 35 dBZ threshold cell positions in 60 minutes using the current ANC growth/decay scheme. The white boundary is the forecasted 35 dBZ threshold cell position in 60 minutes using the ANC growth/decay scheme with total lightning (ANC-LTG). The red boundary represents the NWS Ft. Worth forecast office county warning area.

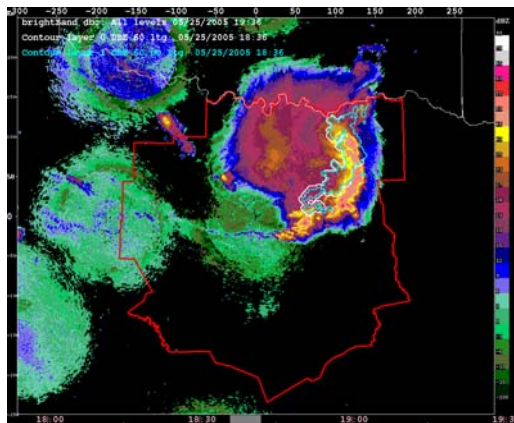


Figure 10. The 60-minute 1836 UTC forecast verification at 1936 UTC on 25 May 2005. The cyan boundaries are the forecasted 35 dBZ threshold cells using the current ANC growth/decay scheme. The white boundaries are the forecasted 35 dBZ threshold cells using the ANC-LTG. The red boundary represents the NWS Ft. Worth forecast office county warning area. Cell growth is well captured in this example, but errors in the extrapolation significantly deteriorated the forecast skill scores at this time.

The ANC fuzzy logic scheme including total lightning (ANC-LTG) provides significant improvement in the POD from 1911 UTC to 2116 UTC (Fig. 11). Despite the overall poor performance of the ANC during the latter stages of this case, the ANC-LTG slightly improves the FAR scores 10 out of 11 forecast periods between 1821 UTC and 1953 UTC (Fig. 12). During the decay stages of the multicell event, the ANC-LTG improved the POD by 9.40%, reduced the FAR by 0.91% and increased the CSI by 2.98% (Fig. 13). The largest source of error leading to CSI values below 0.15 during the decay stage of this case was TITAN's poor extrapolation of the 35 dBZ cells. We emphasize the importance of focusing on the relative improvement of the ANC with total lightning fields, as opposed to the raw quantitative numbers. Acceleration of the squall line's southern flank in the example shown (Fig. 9-10) led to poor performance in the forecast verification scores at and around 1936 UTC. New object-based verification techniques (Halley-Gotway et al., 2005) will alleviate these ANC forecast evaluation problems in the near future.

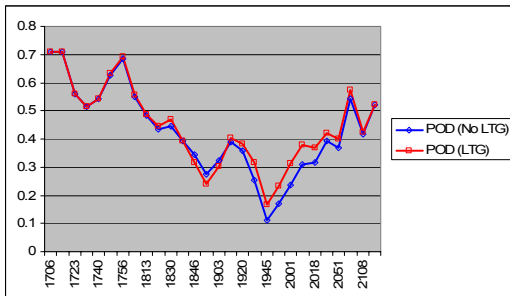


Figure 11. The 25 May 2005 time-series (in UTC) probability of detection (POD) for the ANC's current forecast logic (blue) and the ANC-LTG (red). All times along the abscissa are in UTC.

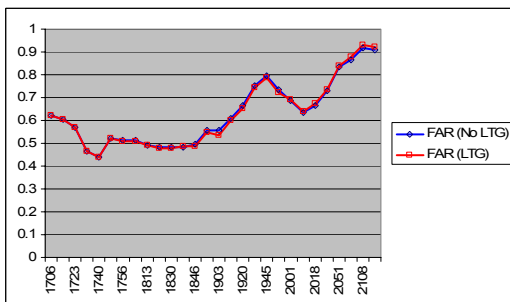


Figure 12. Same as Figure 11, except now for the false alarm ratio (FAR)

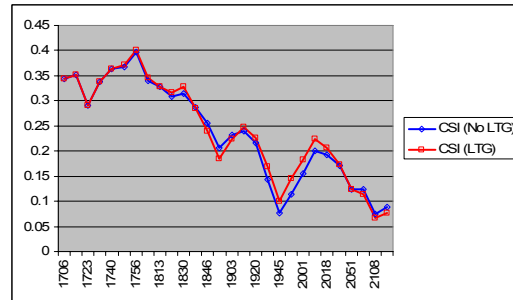


Figure 13. Same as Figure 11, except now for the critical success index (CSI)

6.3 Overall results

The addition of total lightning to the Dallas-Ft. Worth ANC growth/decay forecast logic demonstrates the potential for improved 60-minute nowcasting performance. In our three case studies, the ANC-LTG increased the POD by over 2% on average (See Table 1 for results). The FAR was decreased slightly and the CSI improved by over 0.8% in two of the three cases. The fuzzy logic scheme used with the total lightning for this study was conservative, so it is expected that emphasizing more weight upon the TITAN-derived FED membership functions would further improve 60-minute growth/decay forecasting performance in most instances. Additional case studies should be analyzed to better understand the effects of the total lightning membership functions upon the complex growth/decay forecast component of the ANC. Adjustments to the fuzzy logic weighting and final growth/decay constraints could offer substantially different results. There may also be a total lightning dependence upon mode of convection and performance.

Additional membership functions provide redundancy in the fuzzy logic, and in turn improve ANC forecast output. It is recommended that future evolution of the ANC growth/decay component include radar reflectivity and total lightning derived membership functions when available. Short-term mesoscale NWP and mesonet surface observations should also be considered possible growth/decay forecast components to obtain a better grasp of the in-situ and future environment of ongoing convection, as opposed to the history-weighted trends currently used.

Extrapolation is the most significant source of error in the 60-minute forecast output provided by the ANC. It may be possible to

improve the TITAN 35 dBZ threshold cell motion vectors using the cross-correlation of total lightning cells. However, this introduces other difficulties such as how to handle cells with warm-precipitation processes that lack lightning activity and the range limitations of the LDAR II network. Continued advancement of the ANC's VDRAS boundary-layer model may also provide added benefit toward the extrapolation forecasts with its potential for real-time tropospheric wind analysis in the future.

The integration of LDAR II data into the Dallas-Ft. Worth ANC has shown that total lightning's nowcasting skill is at least on par with WSR-88D radar reflectivity during most scenarios in close proximity (within 100 km) to the network. The next step for NCAR will be the introduction of total lightning into the new ANC forecast demonstration project at White Sands Missile Range (WSMR) in New Mexico. This region is characterized by isolated and electrically active convection. Similar methods discussed in this paper will be utilized to integrate data from the WSMR total lightning mapping array into its ANC installation; with hopes to improve the 0-to-60 minute growth/decay forecast performance.

7. LDAR II LIGHTNING TOP PRODUCT

The inconsistencies in the SCIT radar echo top product used in the WSR-88D network were introduced in Section 3. Demetriades et al. (2003) and Steiger et al. (2005) demonstrated the consistency a "lightning top" product derived from LDAR II VHF sources could provide end-users. Increased storm echo top accuracy would benefit severe thunderstorm nowcasting, terminal area aviation forecasting and flash flood forecasting thanks to its close connection to thunderstorm intensity and evolution.

We now create an LDAR II-derived lightning top product using the Dallas-Ft. Worth supercell case from 25 April 2005 for examination. The lightning top product is created every four minutes by categorizing all VHF sources to their respective 2km x 2km Cartesian grid box. The accumulated VHF source points are ranked by altitude and the 90th percentile altitude source is assigned to the grid box to represent the estimated storm echo top derived from its electrical activity. An example comparison of radar reflectivity, FED and the lightning top product are shown in Figure 14.

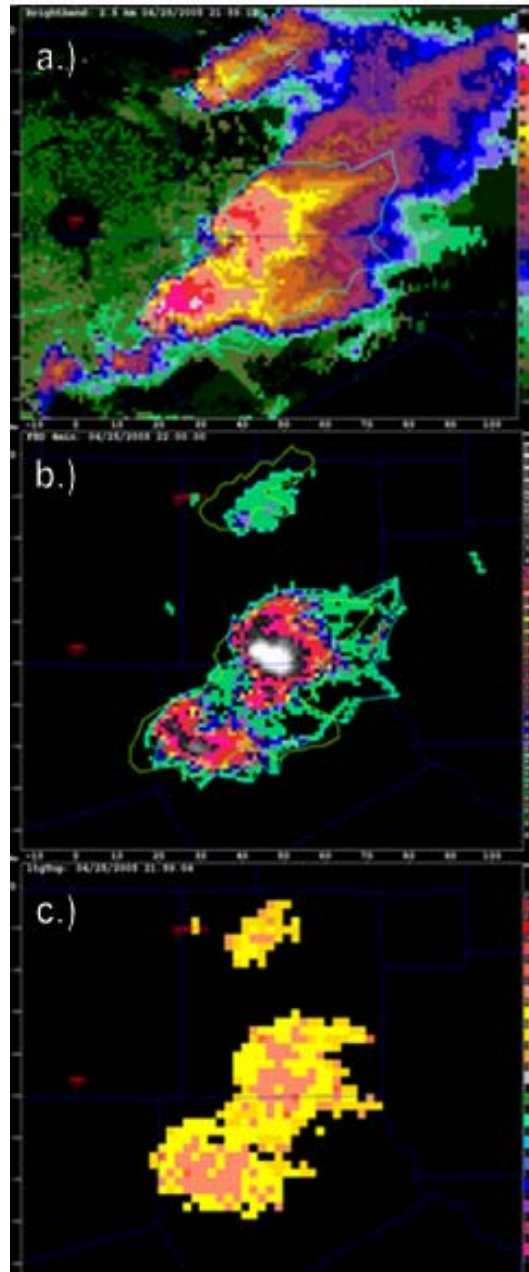


Figure 14. a.) 2.5 km CAPPI of radar reflectivity (dBZ) from the KFWS WSR-88D at 2159 UTC on 25 April 2005. b.) Same window, except now the FED ($\text{flashes km}^{-2} \text{min}^{-1}$) at 2200 UTC. c.) Same window, except now the 90th percentile lightning top (km).

Rather than compare the consistency of the lightning top and SCIT radar echo tops, we instead examine the potential to use lightning top trends to predict thunderstorm growth/decay in a nowcast setting. Similar TITAN-derived attributes are evaluated using the data from three supercells that tracked across the Dallas-Ft. Worth area on 25 April 2005 (Fig. 15).

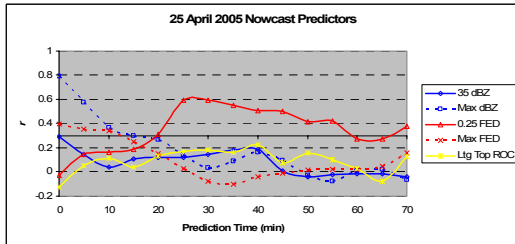


Figure 15. The Pearson linear lag correlation coefficients in 5-min intervals comparing the TITAN 35 dBZ cell NAGR (blue), maximum dBZ (blue-dash), 0.25 FED NAGR (red), maximum FED (red-dash) and lightning top rate of change (yellow) as predictors for the 35 dBZ cell area. The lag correlations are calculated for each of the three supercells on 25 April 2005 and then averaged together at 5-min iterations.

The results of this analysis demonstrate that the lightning top rate of change product does not provide any skill in the prediction of future thunderstorm growth and decay. Its performance is very similar to that of the TITAN-derived 35 dBZ radar reflectivity threshold NAGR. Just as in the overall results, the TITAN-derived 0.25 flashes $\text{km}^{-2} \text{min}^{-1}$ is the superior nowcasting parameter. It demonstrates excellent performance ($r > 0.3$) during the 20-to-60 minute forecast period. It is likely that lightning flash coverage trends are accentuated when tracking discrete supercells, as was the case during this event. TITAN-derived parameter performance as a function of convective mode will be a focus of future work. The identification of favorable parameters for certain storm types could ease the fuzzy logic tuning difficulties encountered when introducing the ANC to new geographic regions.

8. CONCLUSIONS

The emergence of new observational technologies and expert systems is quickly altering the methods in which 0-to-3 hour time- and space-specific forecasts known as nowcasts are formulated. Weather radar is no longer the only observational source to predict the growth, decay and movement of thunderstorms in near real-time. Three-dimensional total lightning mapping offers improved temporal resolution and its trends are closely tied to updraft strength, a key component of precipitation production and severe weather. Expert systems, such as the NCAR ANC, necessitate automated solutions to quickly ingest and provide meaningful output to forecasters. The ANC's TITAN-derived 0.25 flashes $\text{km}^{-2} \text{min}^{-1}$ threshold NAGR is the leading cell trend parameter to predict thunderstorm growth/decay and intensity. The use of historic cell area trends to predict future size and intensity is inherently flawed. But, until computing power allows for "nowcast" numerical weather prediction, TITAN and SCIT cell trending will offer the most successful automated nowcast solution to assist forecasters.

Applications using LDAR II total lightning will continue to be explored. The estimation of thunderstorm echo tops using the 90th percentile VHF source altitudes eliminates the inconsistencies often seen at long ranges with weather radar, but the trend of lightning top heights do not appear to provide added skill to the nowcast. Perhaps lightning mapping array networks that receive higher VHF source counts due to increased sensors and sensitivity would provide improved trend information that could benefit the nowcast process.

It is recommended that the ongoing ANC implementation in Beijing, in preparation for the 2008 Summer Olympics nowcasting demonstration, incorporate two-dimensional total lightning data into the growth/decay and extrapolation fuzzy logic scheme. The presence of a SAFIR interferometric total lightning mapping network allows for the use of similar FED trends to complement the radar reflectivity data.

Event and Storm lifecycle stage	ANC current set-up	ANC-LTG	Change (in %)	ANC current set-up	ANC-LTG	Change (in %)	ANC current set-up	ANC-LTG	Change (in %)
	POD	POD		FAR	FAR		CSI	CSI	
25-Apr									
Overall	0.37021	0.37878	+2.31	0.56406	0.57225	-1.45	0.23549	0.23346	-0.86
Growth	0.30520	0.31411	+2.89	0.51784	0.52048	-0.51	0.20934	0.21182	+1.19
Mature	0.41152	0.41992	+2.04	0.59348	0.60519	-1.97	0.25213	0.24723	-1.94
Decay	N/A	N/A	N/A	N/A	N/A	N/A	N/A	N/A	N/A
25-May									
Overall	0.42823	0.44571	+4.08	0.62834	0.62678	+0.25	0.23731	0.2416	+1.81
Growth	0.58137	0.58534	+0.68	0.52166	0.52090	+0.15	0.34293	0.34493	+0.58
Mature	0.30676	0.32253	+5.14	0.61297	0.60370	+1.51	0.20836	0.21501	+3.19
Decay	0.38863	0.42514	+9.40	0.78088	0.78798	+0.91	0.14147	0.14568	+2.98
1-Jul									
Overall	0.32202	0.32218	+0.05	0.64681	0.64646	+0.05	0.17002	0.17140	+0.81
Growth	0.20473	0.20658	+0.91	0.58773	0.58672	+0.17	0.14221	0.14327	+0.75
Mature	0.25342	0.26678	+5.27	0.52374	0.52673	+1.13	0.19578	0.20442	+4.42
Decay	0.46165	0.45201	-2.09	0.76774	0.77154	-0.49	0.17638	0.17341	-1.69

Table 1. A detailed analysis of the ANC 60-minute forecast skill scores. The first column lists the event date and below that the skill scores are divided into four storm lifecycle sub-sets: Overall – average of every forecast for the entire event, Growth – forecasts as area coverage increased, Mature – forecasts at and around the peak of storm area coverage and Decay – forecasts as the area decreased. The orange colored columns compare the ANC's current growth/decay forecast POD performance to that of the ANC-LTG. The fourth column describes the percentage improvement (+) or degradation (-) in the skill score when using the ANC with total lightning. The yellow and blue columns are the same, analyzing FAR and CSI respectively.

REFERENCES

- Demetriades, N. W. S., M. J. Murphy, and K. L. Cummins, 2002: Early results from the Global Atmospheric, Inc. Dallas-Ft. Worth lightning detection and ranging (LDAR-II) research network. Preprints, 6th Symposium on Integrated Observing Systems, Orlando, FL, Amer. Meteor. Soc., 202-209.
- _____, M. J. Murphy, R. L. Holle, and P. Richard, 2003: The advantages of total lightning over CG lightning for thunderstorm cell identification and tracking and its complements to radar reflectivity. 12th International Conference on Atmospheric Electricity, Versailles, France, IAMAS.
- Dabberdt, W., 2002: The scope and future of nowcasting. *Vaisala News*, **159**, 33-37.
- Dixon, M., and G. Wiener, 1993: TITAN: Thunderstorm Identification, Tracking, Analysis, and Nowcasting—A radar-based methodology. *J. Atmos. Oceanic Technol.*, **10**, 785–797.
- Dotzek, N., H. Hartmut, C. Thery, and T. Fehr, 2001: Lightning evolution related to radar-derived microphysics in the 21 July 1998 EULINOX supercell storm. *Atmos. Res.*, **56**, 335-354.
- Halley-Gotway, J., R. Bullock, B. Brown, 2005: Object-based verification of convective storms for the 2005 Dallas/Ft. Worth AutoNowcaster Demonstration Project. Preprints, 32nd Conference on Radar Meteorology, Albuquerque, NM, AMS.
- Harlin, J. D., T. D. Hamlin, P. R. Krehbiel, R. J. Thomas, W. Rison, and D. Shown, 2000: LMA observations of tornadic storms during STEPS 2000. *Eos Trans. AGU*, **81**, Fall Meet. Suppl., Abstract A52C-25.
- Heidke, P., 1926: Berechnung des Erfolges und der Gute der Windstarkevorhersagen im Sturmwarnungsdienst. *Geografiska Annaler*, **8**, 301-349 (In German).

- Howard, K. W., J. J. Gourley and R. A. Maddox, 1997: Uncertainties in WSR-88D measurements and their impacts on monitoring life cycles. *Wea. Forecasting*, **12**, 166-174.
- Johnson, J. T., P. L. MacKeen, A. Witt, E. D. Mitchell, G. J. Stumpf, M. D. Eilts, and K. W. Thomas, 1998: The Storm Cell Identification and Tracking algorithm: An enhanced WSR-88D algorithm. *Wea Forecasting*, **13**, 263–276.
- Lang, T. J., and S. A. Rutledge, 2002: Relationships between convective storm kinematics, precipitation, and lightning. *Mon. Wea. Rev.*, **130**, 2492-2506.
- Lojou, J. Y., and K. L. Cummins, 2005: On the representation of two- and three-dimensional total lightning information. AMS Preprints, *1st Conference on Meteorological Applications of Lightning Data*, San Diego, CA, Amer. Meteor. Soc., 7pp.
- MacGorman, D., D. Rust, O. van der Velde, M. Askelson, P. Krehbiel, R. Thomas, B. Rison, T. Hamlin, and J. Harlin, 2002: Lightning relative to precipitation and tornadoes in a supercell storm during MEAPRS. Preprints, *21st Severe Local Storms Conf.*, San Antonio, TX, Amer. Meteor. Soc., 423-426.
- MacKeen, P. L., H. E. Brooks, and K. L. Elmore, 1999: Radar reflectivity–derived thunderstorm parameters applied to storm longevity forecasting. *Wea. Forecasting*, **14**, 289-295.
- Maynard, R. H. Commander U. S. N., 1945: Radar and Weather. *J. Atmos. Sci.*, **2**, 214–226.
- Mueller, C., T. Saxen, R. Roberts, J. Wilson, T. Betancourt, S. Dettling, N. Oien, and J. Yee, 2003: NCAR Auto-Nowcast System. *Wea. Forecasting.*, **18**, 545-561.
- Nelson, E. J., S. J. Fano, R. Roberts, W. Bunting, T. Saxen, C. Mueller, H. Cai, A. Crook, D. Meigenhardt, and J. Pinto. Evaluation of the NCAR Thunderstorm Auto-Nowcaster during the NWS Ft. Worth Operational Demonstration. Preprints, *32nd Conference on Radar Meteorology*, Albuquerque, NM, Amer. Meteor. Soc.
- Proctor, D. E., 1991: Regions where lightning flashes began, *J. Geophys. Res.*, **96**, 5099-5112.
- Saunders, C. P. R., 1993: A review of thunderstorm electrification processes. *J. Appl. Meteor.*, **30**, 642-655.
- Steiger, S. M., R. E. Orville, M. J. Murphy, and N. W. S. Demetriades, 2005: Total lightning and radar characteristics of supercells: Insights on electrification and severe weather forecasting. Preprints, *First Conference on the Applications of Lightning Data*, San Diego, CA, Amer. Meteor. Soc.
- Sun, J., and N. A. Crook, 2001: Real-time low-level wind and temperature analysis using WSR-88D data. *Wea. Forecasting.*, **16**, 117–132.
- Wilson, N. L., D. W. Breed, T. R. Saxen, and N. W. S. Demetriades, 2006: The performance analysis of total lightning in NCAR's Auto-Nowcaster. Preprints, *Second Conference on the Applications of Lightning Data*, Atlanta, GA, Amer. Meteor. Soc.